

UNCLASSIFIED

AD NUMBER

AD852601

LIMITATION CHANGES

TO:

Approved for public release; distribution is unlimited. Document partially illegible.

FROM:

Distribution authorized to U.S. Gov't. agencies and their contractors; Critical Technology; MAY 1969. Other requests shall be referred to Air Force Armament Laboratory, ATWG, Eglin AFB, FL 32542. Document partially illegible. This document contains export-controlled technical data.

AUTHORITY

afatl ltr, 4 oct 1972

THIS PAGE IS UNCLASSIFIED

AFATL-TR-69-42

AD852601

Analytic and Experimental Interior Ballistics of Closed Breech Guns

by

Otto K. Heiney, 1st Lt, USAFR

MAY 1969

D D C
REF ID: A652601
MAY 26 1969
B

This document is subject to special export controls,
and each transmittal to foreign nationals or foreign
governments may be made only with prior approval of
the Air Force Armament Laboratory (ATWG), Eglin Air
Force Base, Florida 32542.

AIR FORCE ARMAMENT LABORATORY
AIR FORCE SYSTEMS COMMAND • UNITED STATES AIR FORCE
EGLIN AIR FORCE BASE, FLORIDA

74

ANALYTIC AND EXPERIMENTAL INTERIOR BALLISTICS
OF CLOSED BREECH GUNS

by

Otto K. Heiney, 1st Lt, USAFR

This document is subject to special export controls,
and each transmittal to foreign nationals or foreign
governments may be made only with prior approval of
the Air Force Armament Laboratory (ATWG), Eglin Air
Force Base, Florida 32542.

FOREWORD

This report has been generated under the interior ballistic analysis portion of Project 62405094 2560. It is an extension of a propellant actuated device interior ballistic formulism developed at the Jet Propulsion Laboratory (reference 1) at Pasadena, California, under NAS 7-100. The report was written by 1st Lt O. K. Heiney, USAFR, attached to the Air Force Armament Laboratory [AFATL (ATWG)] for an annual active duty tour. Assistance of the personnel of both AFATL (ATBA) and the Armament Development and Test Center [ADTC (ADTVF-2)] with the formulation and execution of the computer program is gratefully acknowledged.

Information in this report is embargoed under the Department of State International Traffic in Arms Regulations. This report may be released to foreign governments by departments or agencies of the U. S. Government subject to approval of the Air Force Armament Laboratory (ATWG), Eglin Air Force Base, Florida, or higher authority within the Department of the Air Force. Private individuals or firms require a Department of State export license.

This technical report is approved.

CHARLES K. ARPKE, Lt Colonel, USAF
Acting Chief, Weapons Division

ABSTRACT

A closed breech incremental interior ballistic formulism is presented along with a Fortran 4 computer program which utilizes the system. Typical input and output data, both plotted and tabular, are included. A unique characteristic of the system is that it avoids the inaccuracies associated with approximate analytic propellant regression expressions in that regression rates are determined by a tabular routine. Various pressure gradient expressions are investigated. Correlation of the mathematical model and computer predictions to experimental device firings are presented. A shock-driven deflagration effect which may be initiated during the ignition transient is described and a postulated correlation parameter defined.

This document is subject to special export controls, and each transmittal to foreign nationals or foreign governments may be made only with prior approval of the Air Force Armament Laboratory (ATWG), Eglin Air Force Base, Florida 32542.

(The reverse of this page is blank.)

CONTENTS

		Page
	NOMENCLATURE	vii
I.	INTRODUCTION	1
II.	ANALYSIS	2
	Energy Balance	2
	Pressure Gradient and Gas Kinetic Energy	4
	Gas Production	13
III.	COMPUTER PROGRAM	15
	Input Data and Usage	15
	Results	16
	Computer Program	16
IV.	EXPERIMENTAL RESULTS	27
	Normal Deflagration	27
	Shock-Driven Deflagration	31
	REFERENCES	36

ILLUSTRATIONS AND TABLES

Figure

1.	Density Gradient as Function of Shot Velocity	7
2.	δ Value as Function of Projectile Velocity	9
3.	Shot Pressure to Static Pressure Ratio, $T = T_0$	11
4.	Shot Pressure to Static Pressure Ratio, $T = .7T_0$	12
5.	Graph of 20mm Performance 0.015 Web	19
6.	Graph of 20mm Performance 0.020 Web	23
7.	Device to Measure Pressure-Time History and Muzzle Velocity	27
8.	Ignition and Propellant Loading Techniques	28
9.	Pressure Time Plot With $\Delta = 57.0 \text{ in.}^2/\text{in.}^3$	29
10.	Pressure Time Plot With $\Delta = 61.0 \text{ in.}^2/\text{in.}^3$	30
11.	Pressure Time Plot With $\Delta = 65.5 \text{ in.}^2/\text{in.}^3$	30
12.	Pressure Time Plot With $\Delta = 76.7 \text{ in.}^2/\text{in.}^3$	32
13.	Pressure Time Plot With $\Delta = 80.0 \text{ in.}^2/\text{in.}^3$	33
14.	Pressure Time Plot With $\Delta = 82.0 \text{ in.}^2/\text{in.}^3$	33
15.	End Cap After Detonative Reaction	34

ILLUSTRATIONS AND TABLES (CONTINUED)

Table	Page
I. PROGRAM INPUT: TYPICAL PROPELLANT AND CASE DATA CARDS	17
II. COMPUTER PRINTOUT OF 20MM PERFORMANCE 0.015 WEB ...	18
III. COMPUTER PRINTOUT OF 20MM PERFORMANCE 0.020 WEB ...	21
IV. INTERIOR BALLISTIC PROGRAM FORTRAN ⁴ LISTING	24
V. CHARGE CHARACTERISTICS	31

NOMENCLATURE

Λ	= Bore Area
a	= Acceleration
C	= Arbitrary Constant
C_v	= Constant Volume Gas Specific Heat
C_w	= Charge Weight
E_G	= Kinetic Energy of Propellant Gas
F	= Force
F_p	= Impetus of Propellant
g	= Acceleration Due to Gravity
m_A	= Pseudo Mass of Propelled Device
m_p	= Mass of Propelled Device
M	= Mach Number
N_B	= Propellant Burned
P_{AV}	= Average Plenum Pressure
P_o	= Total Pressure
P_s	= Shot Base Pressure
r	= Regression Rate of Propellant
R	= Gas Constant
S_B	= Burning Surface of Propellant
T	= Gas Temperature
T_o	= Isochoric Flame Temperature of Propellant
V	= Shot Velocity
v_c	= Initial Chamber Volume
v	= Gas Velocity
X	= Distance from Shot Base to X_0
X_0	= Initial Shot Reference
x	= Arbitrary Reference Behind Shot
β	= Heat Loss Factor
γ	= Specific Heat Ratio of Propellant Gas
δ	= Density Distribution Factor
η	= Covolume of Propellant Gases
ρ	= Average Density of Gas
ρ_p	= Density of Propellant
ρ_0	= Breech Gas Density
ρ_s	= Density of Gas at Projectile
ϕ	= Pressure Gradient Factor
w_0	= Initial Propellant Web
Δ	= Burning Surface Factor

(The reverse of this page is blank.)

SECTION I

INTRODUCTION

The basic interior ballistic problem of any closed breech gun system is to determine the energy release and corresponding pressure generated by the burning of propellant in a variable volume. From the energy balance and the equation of state, the pressure-time or pressure-travel as well as muzzle velocity and piezometric efficiency of the system is established, thus providing the complete ballistic solution.

The results of the analysis, Section II, are essentially contained in equations (9) and (26) which are in an incremental form specifically tailored for machine computation. Program listing and typical results are presented in Section III.

The analysis in Section II considers first the energy balance of the system in paragraph A, Section II. In paragraph B, Section II, the kinetic energy in the propellant gas is determined. Also investigated are various expressions for the pressure gradient from the breech to the moving shot. In paragraph C, Section II, the constant burning surface of single perforate propellant is demonstrated and a tabular regression routine defined.

Section IV illustrates the comparison of the presented model to experimentally measured pressure histories of device firings. The experimental set-up is described, and a shock-driven deflagration phenomenon that was encountered is defined.

SECTION II

ANALYSIS

ENERGY BALANCE

The Noble-Abel equation of state is:

$$P(V - \gamma) = nRT \quad (1)$$

Where γ is the "covolume" of the propellant and has the units of volume/mass which arises due to the fact that the combustion products are not perfect gases.

The central property of the propellant is its "impetus," F_p , which is qualitatively similar to the c^* of rocket propellants.

$$F_p = RT_0 \quad (2)$$

Where T_0 is the isochoric flame temperature of the propellant gases and F_p has units of specific energy (ft-lb/lb).

The energy equation, following the techniques in reference 2, for the system will be

$$E_1 = E_2 + E_3 + E_4, \text{ where}$$

E_1 = energy put in system from propellant combustion

E_2 = translational energy of piston

E_3 = heat loss to walls

E_4 = kinetic energy of unburned propellant and propellant gases

A = cross section of bore

V_c = initial chamber volume

X = distance from X_0 to piston base.

The instantaneous free chamber volume is a function of the initial chamber volume plus the barrel volume exposed by shot motion minus volume occupied by unburnt propellant and combustion gases. Combining equations (1) and (2) then gives

$$P \left[(V_c + AX) - \frac{(C_w - N_b)}{\rho_p} - \gamma N_b \right] = \frac{N_b F_p T}{T_0} \quad (3)$$

Thermal and chemical energy released by propellant will be

$$E_1 = N_b C_v (T_o - T) \quad (4)$$

Translational energy of the piston will be

$$E_2 = 1/2 m_p v^2$$

The heat loss of the gases is proportional to the distance traveled, which (following reference 3) is roughly proportional to the square of the velocity. We can, to a good approximation, say that

$$E_3 = 1/2 \beta m_A v^2$$

Using the expression developed in paragraph B, below, for the kinetic energy contained in the accelerating gas and unburned propellant, we may write

$$E_4 = 1/2 \frac{C_w v^2}{g \delta}$$

We may define

$$m_A = m_p + \frac{C_w}{\delta g}$$

Then

$$E_2 + E_3 + E_4 = (1 + \beta) (1/2) m_A v^2 \quad (5)$$

Defining Y by equation (6)

$$(Y - 1) = \frac{R}{C_v} = F_p / C_v T_o \quad (6)$$

Then from equations (4), (5), and (6)

$$N_b F_p (1 - T/T_o) = 1/2 (Y - 1) (1 + \beta) m_A v^2 \quad (7)$$

The temperature ratio is eliminated by the introduction of the equation of state to give the fundamental ballistic equation

$$N_b F_p - (\gamma - 1) (1 + \beta) \frac{m_A}{2} v^2 = P_{AV} \left[(v_c + Ax) - \frac{(C_w - N_b)}{\rho_p} - TN_b \right] \quad (8)$$

or as a differential form of equation (8) is more convenient for incremental computation, differentiating, and taking differential chamber volume changes due to charge regression as second order; this is

$$\frac{dP_{AV}}{dt} \left[(v_c + Ax) - \frac{(C_w - N_b)}{\rho_p} - TN_b \right] = \frac{dN_b}{dt} F_p - (\gamma - 1)(1 + \beta) m_A \frac{dv}{dt} \frac{dx}{dt} - P_{AV} A \frac{dx}{dt} \quad (9)$$

Equation (9) provides the basis for the complete incremental interior ballistic solution; however, two additional functions are necessary to provide required relationship in the above formulation.

The first is projectile velocity as a function of average chamber pressure, or $V = f(P_s, t, m_p)$

This relation is determined in paragraph B below. The second expression required is a value for the surface exposed to burning as a function of web fraction burned.

$$N_t = f(P_{AV}, t)$$

which is covered in paragraph C below.

PRESSURE GRADIENT AND GAS KINETIC ENERGY

The determination of the pressure gradient in the barrel is central to the ballistic solution, as the velocity of the shot is a function of the pressure at the shot while equation (9) gives a value for P_{AV} . The density distribution in the gas is also required to give a value for the gas kinetic energy. The density and pressure variations are determined for an average temperature in the combustion chamber of T_0 and also for an average temperature of $7/10 T_0$. This problem was first studied by La'Grange and his approach introduces the analysis.

$$\frac{\partial \rho}{\partial t} + \frac{\partial}{\partial x} (\rho v) = 0 \quad (10)$$

and assuming constant density

$$\frac{\partial \rho}{\partial x} = 0$$

results in equation (10) being separable with the result.

$$\frac{1}{\rho} \frac{\partial \rho}{\partial t} = - \frac{\partial v}{\partial x} = C \quad (11)$$

Equation (11) is integrated with the boundary conditions

$$BD 1. \quad x = X_0 = 0, \quad v = 0$$

$$BD 2. \quad x = X, \quad v = V = \frac{dx}{dt}$$

$$\int_0^V dv = C \int_0^X dx$$

$$v = Cx \quad (12)$$

at boundary 2

$$C = \frac{1}{X} \frac{dx}{dt}$$

then

$$v = \frac{x}{X} \frac{dx}{dt} \quad (13)$$

It is thus seen the constant density assumption of La'Grange will directly result in a linear velocity profile for the gases, equation (13). Constant density is then a sufficient condition for velocity linearity, though not necessarily a necessary condition.

The kinetic energy in the gas using the above approach is then

$$E_G = 1/2 \int_0^X A \rho v^2 dx = \frac{A \rho}{2} V^2 \int_0^X \frac{x^2}{X^2} dx = (1/2) (1/3) A \rho X V^2$$

but

$$A \rho X = \frac{C_w}{g}$$

then

$$E_G = (1/2) (1/3) \frac{C_w V^2}{g} = 1/2 \frac{C_w V^2}{\delta g} \quad (14)$$

where

$\delta = 3$ for the La'Grange solution.

The factor δ was introduced by Hirschfelder (reference 3) in his extension of the work of Kent (reference 4) who allowed the gas density to vary and solved for δ as a function of the charge to projectile mass ratio.

Solutions of the form $\delta = f(C_w/m_p g)$

are useful for the approximate closed form ballistics of Hirschfelder but are of less utility for incremental computer solvable interior ballistic system discussed here. The results of La'Grange ($\delta = 3$) essentially state that the energy in the accelerating gas is equivalent to $1/3$ of the gas mass traveling at shot velocity. This is a good approximation at velocities where the gas density is almost constant. It falls apart, as would be expected, at velocities where the density is no longer uniform.

For incremental computations, δ is most effectively formulated as a function of shot velocity. To do this, it is first necessary to describe the density variation behind the projectile as a function of shot velocity. It is then assumed that a linear velocity gradient exists behind the shot and also that isentropic flow relations may be used during an interval to describe the flow behind the shot.

This requires that the flow during the short interval considered be looked upon as "quasi-isentropic." From reference 5, the density ratio is then

$$\rho/\rho_0 = \left(1 + \frac{\gamma - 1}{2} \frac{v^2}{gRT}\right)^{-1/\gamma} \quad (15)$$

The question then arises as to what temperature should be used to define the speed of sound in the environment of the burning gases. An upper bound for this temperature would be the isochoric flame temperature of the gases T_o ; a reasonable lower bound would be $7/10 T_o$. The analysis is then conducted with the above values as bounds.

The results of equation (15) are plotted on Figure 1 for a $\gamma = 1.222$ and an $RT_o = 375,000 \text{ ft-lb/lb}$.

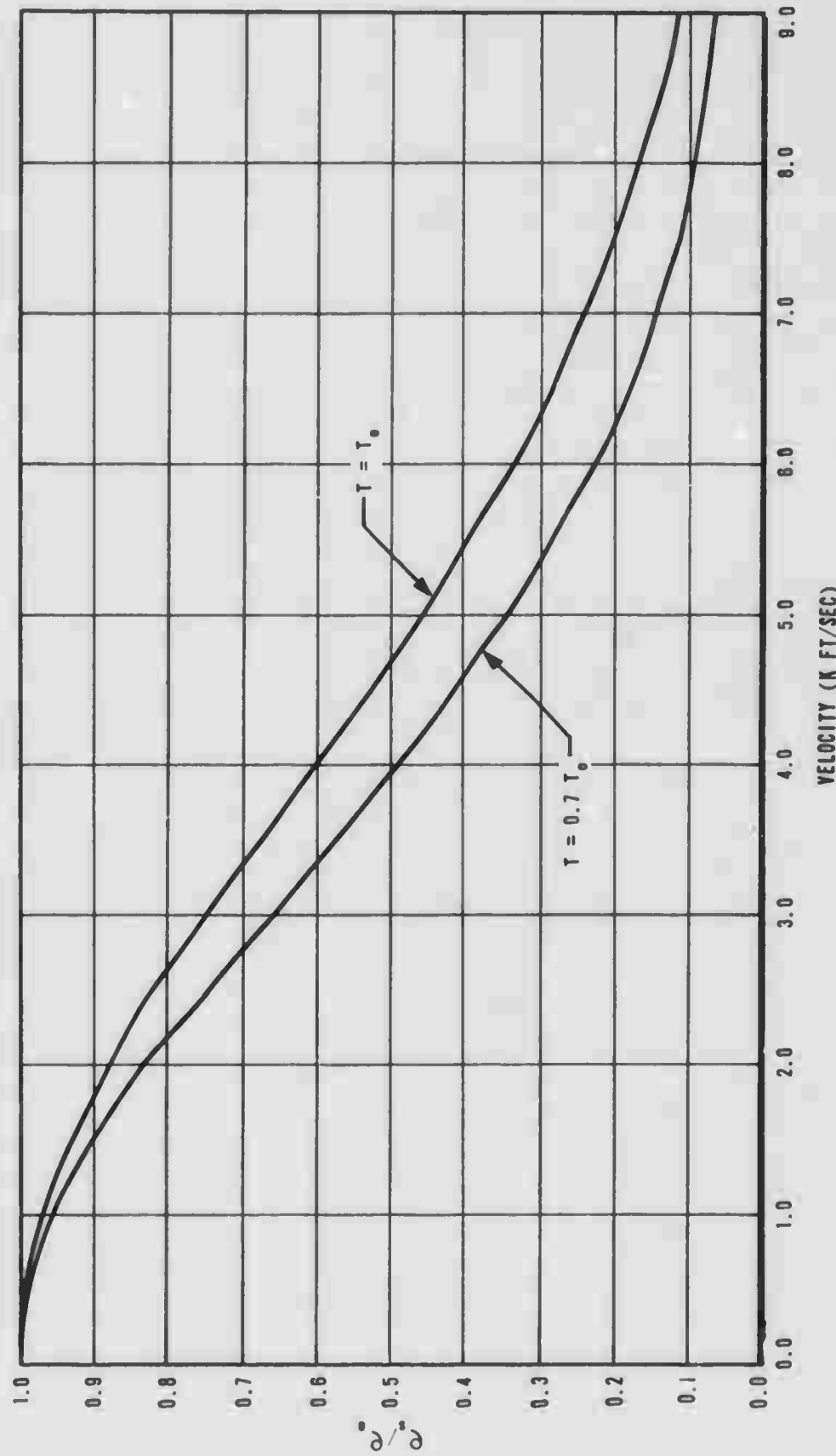


Figure 1. Density Gradient as Function of Shot Velocity.

The energy increment in a small control volume of gas will then be

$$E_I = 1/2 \rho_N v_N^2 A \Delta X_N$$

$$E_G = \frac{A \rho_0}{2} \sum \frac{\rho_N}{\rho_0} v_N^2 \Delta X_N = 1/2 \frac{C_w}{g \delta} v^2 \quad (16)$$

The value of δ , for a given velocity, is determined by performing the numerical summation of equation (16) on a digital computer. The results of this procedure are plotted on Figure 2. As would be expected at low velocities, the value of δ approaches 3.0. The results of δ as a function of velocity is then fed into the main ballistic program as data and allows for the computation of the value of the kinetic energy of the gas.

PRESSURE GRADIENT

The necessity of relating $P_s = f(P_{AV})$ has been explained above. The approach used here is to relate P_s to P_0 by two independent methods and then empirically determine a P_{AV} to P_s relationship. A value for the ratio of P_s/P_0 may be obtained by means of the "quasi-isentropic" assumption used for densities above.

$$\frac{P}{P_0} = \left(1 + \frac{\gamma - 1}{2} \frac{v^2}{gRT} \right)^{-\gamma/\gamma-1} \quad (17)$$

The results of this relation are plotted on Figures 3 and 4 for the temperatures $T = T_0$ & $T = .7T_0$ respectively.

Another approach to the pressure gradient solution would be to assume a constant temperature process. In which case Euler's equation and the equation of state will give:

$$P = \rho RT \quad (18)$$

$$vdv = - \frac{dp}{\rho} \quad (19)$$

combining equations (18) and (19) and integrating

$$\int_0^V vdv = - \int_{P_0}^{P_s} \frac{RT}{P} dP$$

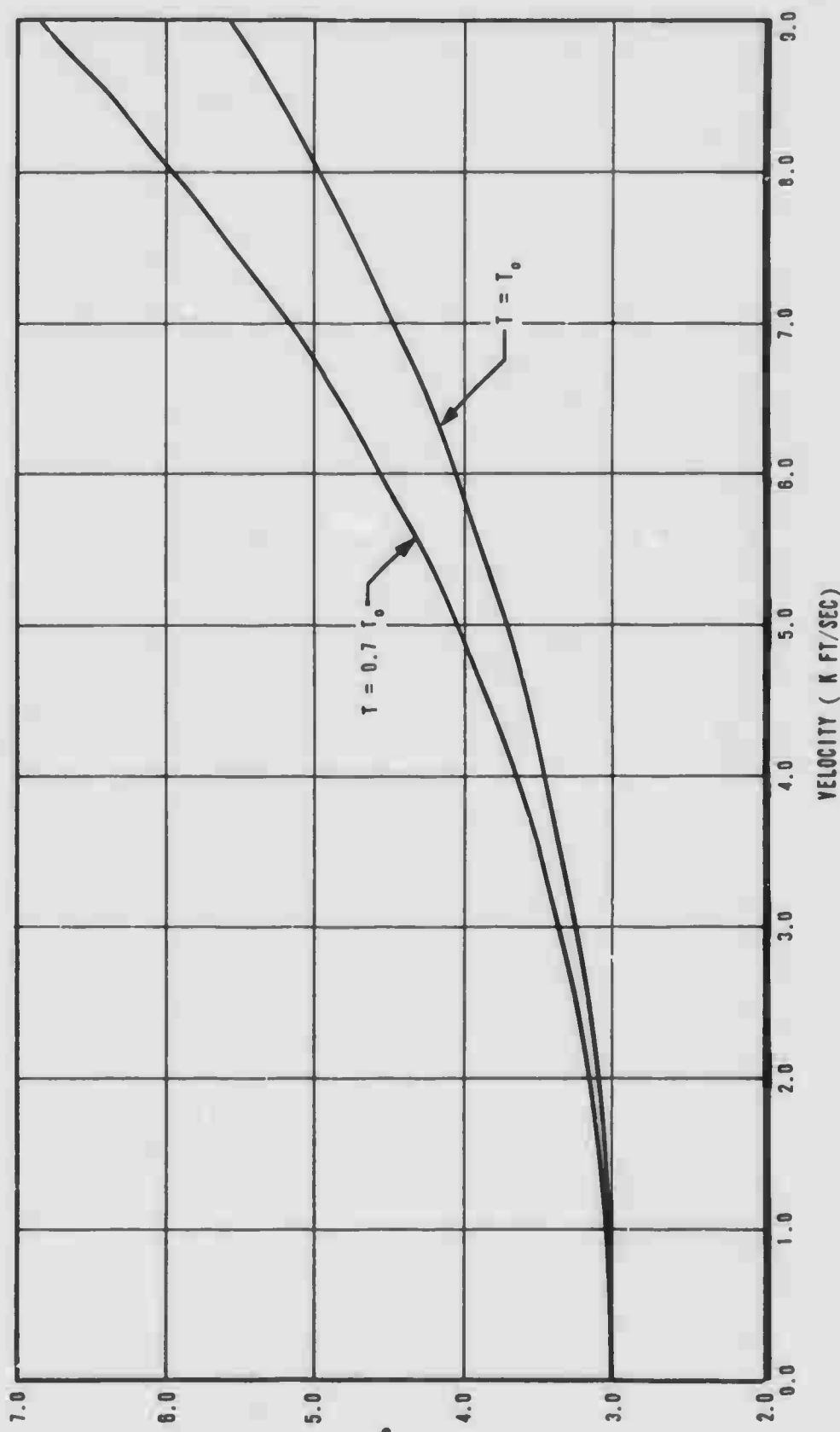


Figure 2. δ Value as Function of Projectile Velocity.

$$\frac{v^2}{2} = -RT \ln (P_s - P_0) \quad (20)$$

The results of equation (20) are also plotted on Figures 3 and 4. The constant temperature equation predicts a lower shot pressure than the quasi-isentropic relation. To relate P_s to P_{AV} then, a heuristically reasonable approach would be to assume that a relation of the form

$$P_s/P_{AV} = \left(1 + \frac{\gamma-1}{2\phi} \frac{v^2}{gRT} \right)^{-\gamma/\gamma-1} \quad (21)$$

with $\phi > 1$ would be satisfactory. To investigate this possibility, it is necessary to develop a value for P_{AV} which has only the gas acceleration energy accounted for. This is done as follows:

$$P_0 v_c - \frac{mv^2}{2\delta} = P_{AV} v_c$$

$$P_{AV}/P_0 = 1 - \frac{v^2}{2\delta gF_p(T/T_0)} \quad (22)$$

Using the expression developed for $\delta = f(v)$ with $\phi = 1.5$ the combined results of equations (21) and (22) will give a value for P_s/P_0 which is again plotted on Figures 3 and 4. It is seen that this value of ϕ gives consistent results for both temperature extremes. It is used in the interior ballistic formulism to relate the average pressures generated by equation (9) to the pressure at the base of the shot required for the equation of motion, as shown below.

$$V = V_0 + at \quad (23)$$

$$a = \frac{P_s A}{m_p} \quad (24)$$

$$P_s = \left[1 + \frac{\gamma-1}{2\phi} M^2 \right]^{-\gamma/\gamma-1} P_{AV} \quad (25)$$

then

$$V = V_0 + \frac{A P_{AV}}{m_p} \left[1 + \frac{(\gamma-1)}{3} \frac{v^2}{g F_p} \right]^{-\gamma/\gamma-1} \quad (26)$$

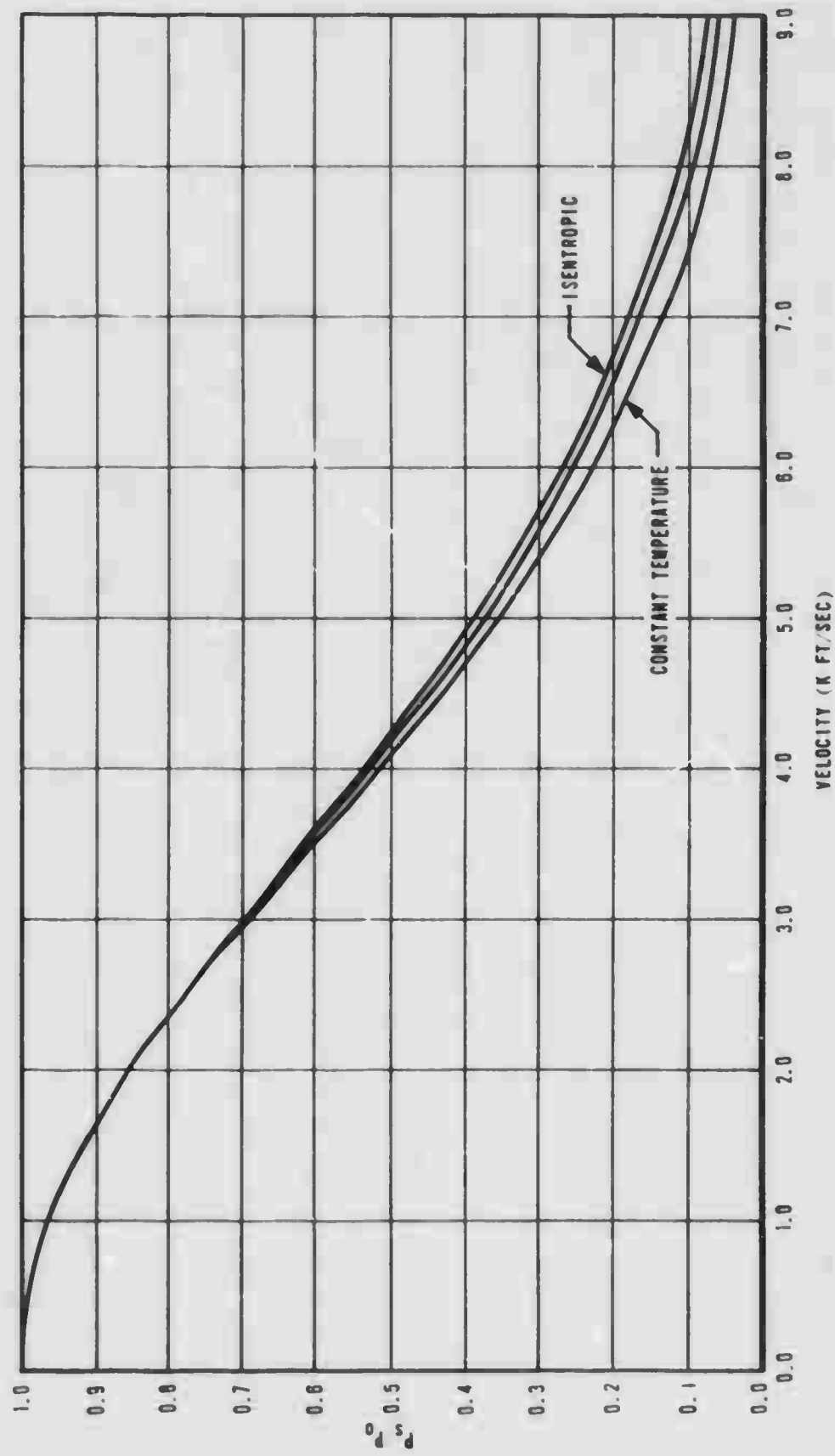


Figure 3. Shot Pressure to Static Pressure Ratio, $T = T_0$.

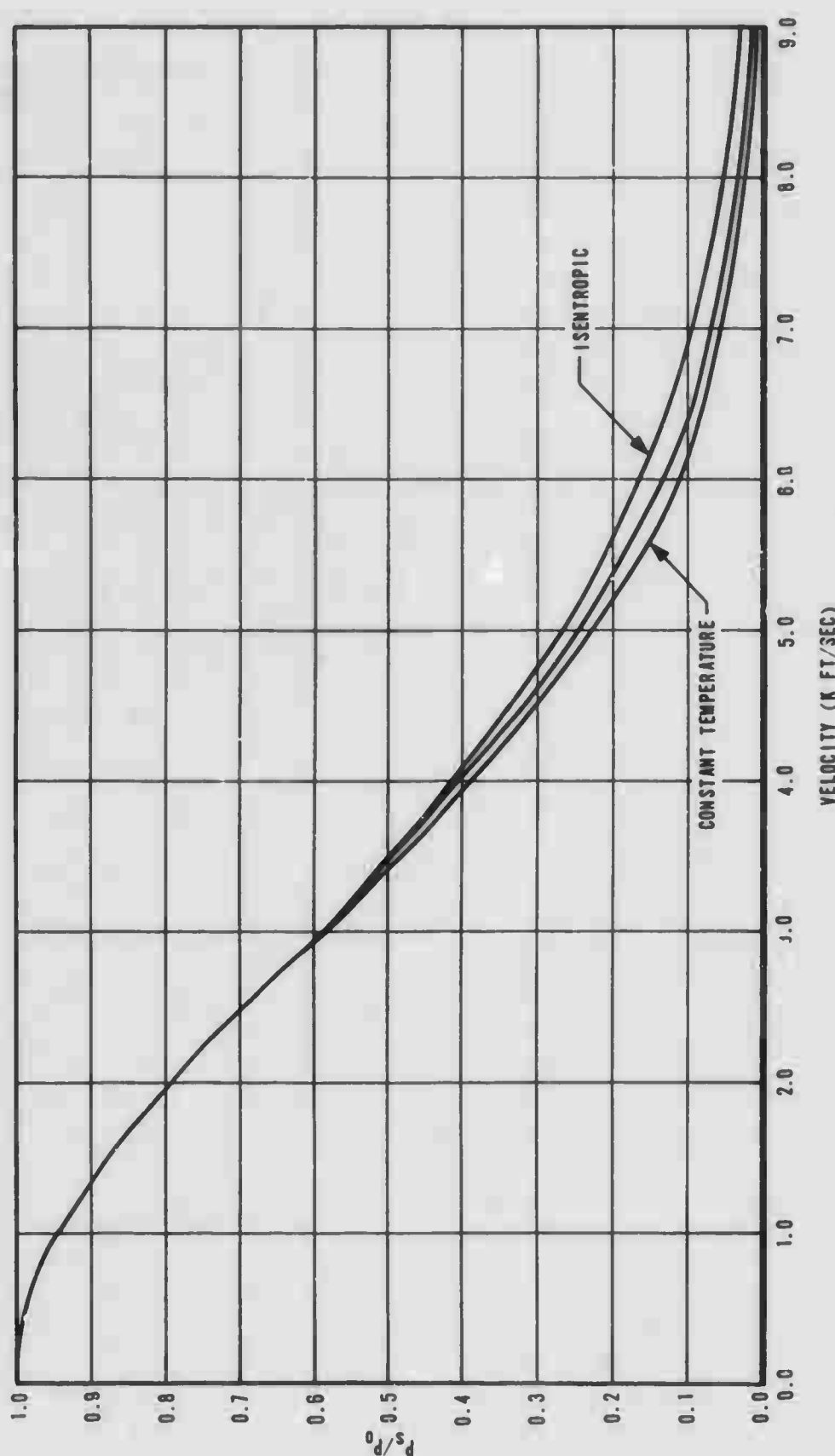


Figure 4. Shot Pressure to Static Pressure Ratio, $T = 0.7T_0$

Equation (26) thus provides the necessary relationship to solve for the projectile motion once the average chamber pressure is shown. The final information required is an expression for the total rates of combustion.

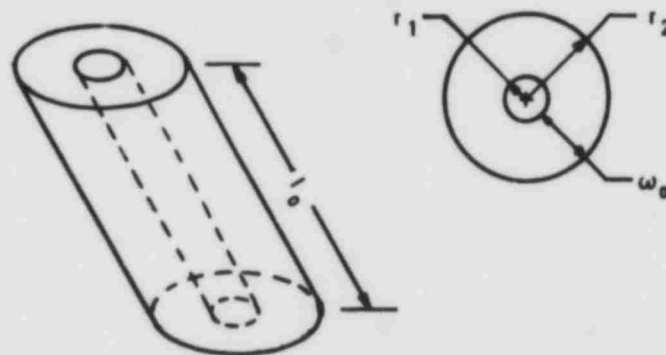
GAS PRODUCTION

The time rate of gas production is simply written as

$$\frac{dN_B}{dt} = r S_B \rho_p$$

In most prior interior ballistic formulisms the approximation $r = BP^n$ with constant N has been made. Frequently, for closed form solutions, the often questionable assumption that $N = 1$ is made. For a numeric solution, however, no approximations are required. Burning rates as a function of pressure, for currently used propellants, are tabulated in reference 7. These values are read into the program as data, and a tabular interpolation routine in the program determines the correct burning rate. Thus all recourse to Vielle's law has been avoided.

The surface of burning of single perforate propellants is very nearly constant as shown below. For other forms, such as cord, disk, and multiperforate, various empirical "form" functions exist to evaluate burning surface as a function of unburned web. These functions are covered in detail in references 3, 6, and 8.



$$w_0 = r_{a,0} - r_{i,0} \quad \text{for a propellant with } \frac{w_0}{l_0} \ll 1.$$

Burning surface for each grain will be

$$S_{I,0} = 2l_0 \pi (r_2 + r_1)$$

after a burning increment of Δr

$$S_{I,t} = 2 l_0 \pi \left([r_2 - \Delta r] + [r_1 + \Delta r] \right) = 2 l_0 \pi (r_2 + r_1)$$

thus at all times the burning surface is constant.

$$\text{Volume of grain} = l_0 \pi (r_2^2 - r_1^2)$$

$$N' = \text{Number of grains/unit mass}$$

Then the burning surface/unit mass of the propellant will be

$$\frac{S_B}{C_w} = \frac{S_I N'}{\rho_p V_0 N'} = \frac{2 l_0 \pi (r_2 + r_1)}{\rho_p l_0 \pi (r_2 - r_1) (r_2 + r_1)} = \frac{2}{\rho_p w_0}$$

or

$$S_B = \frac{2}{\rho_p w_0} C_w \quad (27)$$

Thus equations (9), (26), and (27) plus burning rate data provide the relationships necessary to solve for peak pressure, muzzle velocity and complete pressure-time, pressure-travel, and velocity-travel of any type of closed breech weapon.

SECTION III
COMPUTER PROGRAM

INPUT DATA AND USAGE

The input data for the program is in two parts. The first is the burning rate and impetus data for the propellant and may remain unchanged as long as one type of propellant is used. The second type card delineates the exact parameters for one given case and will change for each case. Propellant data are determined from the tables in references 7 and 9.

PROPELLANT CARDS.

1st CARD

Columns	Data	Decimal Point	Units
1-8	Impetus of Propellant	7	Ft-Lb/Lb
12-16	Specific Heat Ratio of Gases	13	Dimensionless
20-24	Density of Propellant	20	Lb/In. ²
28-31	Covolume of Gases	30	In. ³ /Lb
33-36	Propellant Type		Alpha Meric

2nd AND 3rd CARDS

20 reference pressures - 10 per card from 500 to 200,000 psia.

4th AND 5th CARDS

20 burning rates taken from reference 7 at pressures listed above.

6th AND 7th CARDS

20 reference velocities taken from 0 to 12,000 ft/sec.

8th AND 9th CARDS

Density distribution factor appropriate to propellant used and corresponding to velocity listed above. Values can be extracted from Figure 2.

PROBLEM CARDS.

Columns	Data	Decimal Point	Units
1-7	Bore Area	4	In. ²
8-14	Chamber Volume	11	In. ³
15-21	Projectile Weight	19	Lb
22-28	Barrel Length	27	In.
29-35	Propellant Web	31	In.
36-42	Heat Loss	40	Dimensionless
43-49	Charge Weight	44	Lb
50-56	Shot Start Press	56	Lb/In. ²

As many problem cards as desired may be loaded after the data for a given propellant and will be handled sequentially by the program. Data in the above format is illustrated in Table I.

RESULTS

Typical output is illustrated in Figures 5 and 6 and Tables II and III. Output includes time from propellant ignition, chamber pressure, shot base pressure, projectile velocity, chamber pressure slope, and distance traveled for a typical 25mm. The two sample cases are identical except for a decrease in charge weight in the latter. Subsequent to the case run, additional computations of extrapolated muzzle velocity to the specified barrel length, ballistic efficiency, and piezometric efficiency are also made. Following each printed output is the pressure-travel plot generated by the computer, which is also a standard output. It should be noted that the program is currently set up to run single perforate uninhibited propellant. For other forms, a proper form function, as mentioned above, must be inserted in the program. The heat loss factor, θ , has a value of between .3 to .4 for a 25mm and will be somewhat larger for smaller bores and less for larger bore weapons.

COMPUTER PROGRAM

The FORTRAN Program listing used is given as Table IV. Run time on the 7094 computer is quite short (about .05 second per case). The program number is 958, and it is being maintained by ADTC (ADTVF-2).

TABLE I. PROGRAM INPUT: TYPICAL

BT: TYPICAL PROPELLANT AND CASE DATA CARDS.

TABLE II. COMPUTER PRINTOUT OF 20NM PERFORMANCE 0.015 WEB.

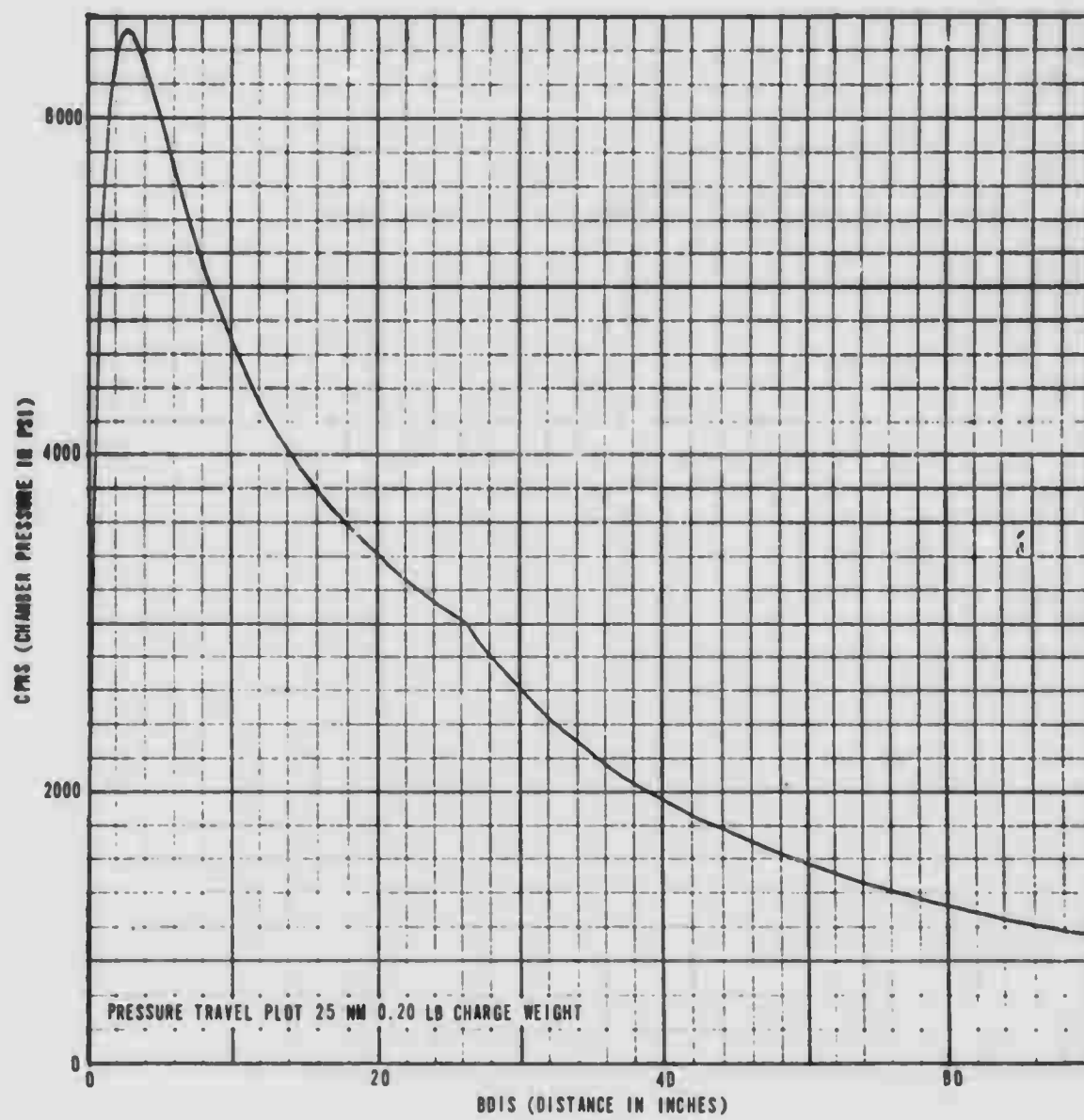


Figure 5. Graph of 20mm Performance 0.015 Web.

19 (The reverse of this page is blank.)

TABLE III. COMPUTER PRINTOUT OF 20NM PERFORMANCE 0.020 WEB.

Serial No.	Crashif	WFM	W.LENGTM	CMB VOL HUNDE AREA	TIME	CRASHI PHRS	THAVFL	PNUP HUNDED	PRES SLOPE	VELOCITY	HS PHRS
•0000	•0000	•000	•000	•000	•001	•001	•001	•0027	29660546.3	6.17	•0000.0
•0000	•0000	•000	•000	•000	•002	•002	•002	•0059	30139304.6	13.48	•741.0
•0001	•0001	•000	•000	•000	•003	•003	•003	•0095	3955022.5	22.10	•594.5
•0001	•0001	•000	•000	•000	•004	•004	•004	•0138	45665751.5	32.25	•683.3
•0001	•0001	•000	•000	•000	•005	•005	•005	•0146	5178H485.4	44.15	•719.8
•0001	•0001	•000	•000	•000	•006	•006	•006	•0242	59071.11.1	58.05	•914.3
•0002	•0002	•000	•000	•000	•007	•007	•007	•0305	66698321.2	74.22	•0490.6
•0002	•0002	•000	•000	•000	•008	•008	•008	•0376	72872565.5	92.45	•12152.1
•0002	•0002	•000	•000	•000	•009	•009	•009	•0452	7941150A.7	114.49	•13472.3
•0002	•0002	•000	•000	•000	•010	•010	•010	•0542	H5970003.4	139.04	•15454.9
•0003	•0003	•000	•000	•000	•011	•011	•011	•0638	92380045.9	167.00	•1M10U.0
•0003	•0003	•000	•000	•000	•012	•012	•012	•0749	98556620.7	198.45	•204U2.0
•0004	•0004	•000	•000	•000	•013	•013	•013	•0845	1050940U.4	233.69	•22856.4
•0004	•0004	•000	•000	•000	•014	•014	•014	•0994	110832946.5	272.95	•25469.2
•0004	•0004	•000	•000	•000	•015	•015	•015	•1138	11504W45.7	316.45	•2H216.1
•0004	•0004	•000	•000	•000	•016	•016	•016	•1294	117065760.1	364.36	•31074.5
•0004	•0004	•000	•000	•000	•017	•017	•017	•1461	1101217553.1	416.71	•33458.3
•0004	•0004	•000	•000	•000	•018	•018	•018	•1634	110128894.4	473.40	•36769.9
•0005	•0005	•000	•000	•000	•019	•019	•019	•1942	103277387.3	534.21	•39444.7
•0005	•0005	•000	•000	•000	•020	•020	•020	•2022	92195H49.9	598.H6	•41937.1
•0005	•0005	•000	•000	•000	•021	•021	•021	•2224	H0477086.9	666.41	•44140.6
•0005	•0005	•000	•000	•000	•022	•022	•022	•2433	06976117.0	737.85	•66125.5
•0006	•0006	•000	•000	•000	•023	•023	•023	•2646	528312Yn.0	811.11	•75223.3
•0006	•0006	•000	•000	•000	•024	•024	•024	•28621883.1	H86.1J	•8H657.2	
•0006	•0006	•000	•000	•000	•025	•025	•025	•30HJ	24454665.1	462.31	•49416.8
•0006	•0006	•000	•000	•000	•026	•026	•026	•3305	11179920.5	1039.11	•49814.5
•0007	•0007	•000	•000	•000	•027	•027	•027	•3527	333017.4	1116.00	•49817.2
•0007	•0007	•000	•000	•000	•028	•028	•028	•3750	-980462.7	1142.53	
•0007	•0007	•000	•000	•000	•029	•029	•029	•2H63	38621883.1	1162.15	
•0007	•0007	•000	•000	•000	•030	•030	•030	•30KJ	24454665.1	1268.29	
•0007	•0007	•000	•000	•000	•031	•031	•031	•3107	25963059.4	1342.95	
•0007	•0007	•000	•000	•000	•032	•032	•032	•3128109.7	4416.25		
•0007	•0007	•000	•000	•000	•033	•033	•033	•355579106.4	1487.98		
•0007	•0007	•000	•000	•000	•034	•034	•034	•3H41	-3H664249.1	1557.98	
•0007	•0007	•000	•000	•000	•035	•035	•035	•3750	-1852847.0	1626.15	
•0007	•0007	•000	•000	•000	•036	•036	•036	•3972	-1271.7	1626.15	
•0007	•0007	•000	•000	•000	•037	•037	•037	•4192	-25963059.4	1626.15	
•0007	•0007	•000	•000	•000	•038	•038	•038	•4411	-3128109.7	1626.15	
•0007	•0007	•000	•000	•000	•039	•039	•039	•4627	-355579106.4	1687.98	
•0007	•0007	•000	•000	•000	•040	•040	•040	•4841	-3H664249.1	1757.98	
•0007	•0007	•000	•000	•000	•041	•041	•041	•5052	-40761914.1	1826.15	
•0007	•0007	•000	•000	•000	•042	•042	•042	•5260	-41984575.4	1892.44	
•0007	•0007	•000	•000	•000	•043	•043	•043	•5475	-42509476.2	1756.H1	
•0007	•0007	•000	•000	•000	•044	•044	•044	•5666	-42478766.4	1714.27	
•0007	•0007	•000	•000	•000	•045	•045	•045	•5865	-42013644.1	1879.83	
•0007	•0007	•000	•000	•000	•046	•046	•046	•6060	-4122MHU3.4	1938.54	
•0007	•0007	•000	•000	•000	•047	•047	•047	•6252	-40180924.4	1995.45	
•0007	•0007	•000	•000	•000	•048	•048	•048	•6464	-41984575.4	2049.1	
•0007	•0007	•000	•000	•000	•049	•049	•049	•6675	-42509476.2	2156.H1	
•0007	•0007	•000	•000	•000	•050	•050	•050	•6886	-42478766.4	2050.60	
•0007	•0007	•000	•000	•000	•051	•051	•051	•7096	-42013644.1	2104.04	
•0007	•0007	•000	•000	•000	•052	•052	•052	•7296	-4122MHU3.4	2165.93	
•0007	•0007	•000	•000	•000	•053	•053	•053	•7496	-40180924.4	2206.21	
•0007	•0007	•000	•000	•000	•054	•054	•054	•7696	-41984575.4	22618.3	
•0007	•0007	•000	•000	•000	•055	•055	•055	•7896	-42509476.2	231045.7	
•0007	•0007	•000	•000	•000	•056	•056	•056	•8096	-42478766.4	2302.35	
•0007	•0007	•000	•000	•000	•057	•057	•057	•8296	-42013644.1	2348.32	
•0007	•0007	•000	•000	•000	•058	•058	•058	•8496	-4122MHU3.4	2392.94	
•0007	•0007	•000	•000	•000	•059	•059	•059	•8696	-40180924.4	23631.04	
•0007	•0007	•000	•000	•000	•060	•060	•060	•8896	-41984575.4	23641.9	
•0007	•0007	•000	•000	•000	•061	•061	•061	•9096	-42509476.2	2478.62	
•0007	•0007	•000	•000	•000	•062	•062	•062	•9296	-42478766.4	2514.64	
•0007	•0007	•000	•000	•000	•063	•063	•063	•9496	-42013644.1	25434.04	
•0007	•0007	•000	•000	•000	•064	•064	•064	•9696	-4122MHU3.4	25722.7	
•0007	•0007	•000	•000	•000	•065	•065	•065	•9896	-40180924.4	2636.60	

A

(The

(The reverse of this page is blank.)

21

卷之三

MINING AND METALLURGY 15 2010 2 2010 2010

PIT FLOOR WILDLIFE INFLUENCE ON HUNTING EFFICIENCY 11

CORRECTED PRACTICAL EFFICIENCY IS 91.7 PERCENT

198 | ISLAMIC EDUCATION IN AFRICA

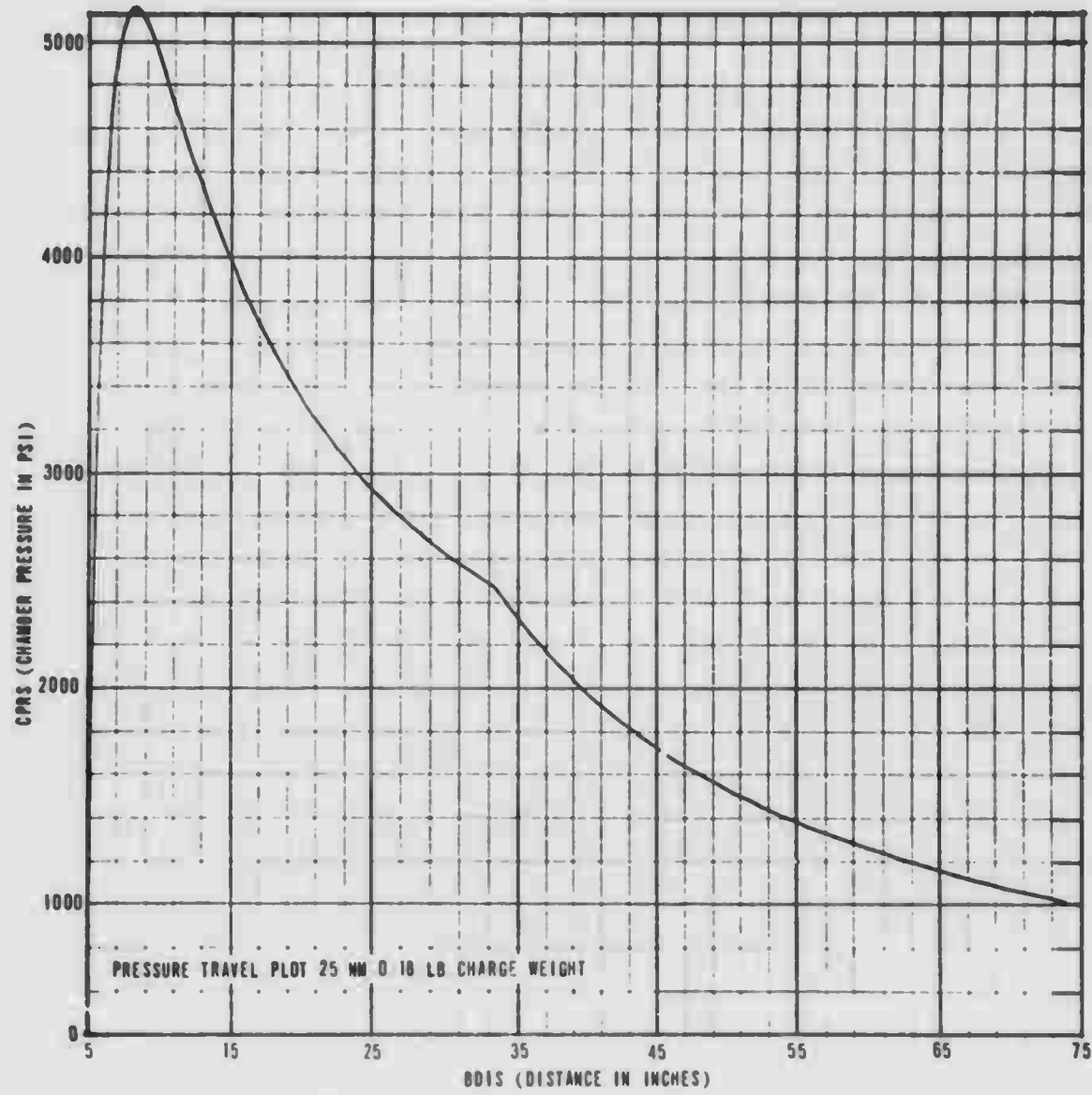


Figure 6. Graph of 20mm Performance 0.020 Web.

TABLE IV. INTERIOR BALLISTIC PROGRAM FORTRAN 4 LISTING.

```

M11580.0
P10P=3000.
CPMS=CPHS
GAMMA=(1.0+HETA)*(GAMA-1.0)
DO 34 J=1,750,1
34 J=1
    7A :CPMS=PHS(JA) 77,16,75
    7S JA+1
      60 IN 7H
    7A H RATE(JA)
      60 TO 10
    77 UTCPMS(JA)=PHS(JA-1)
      DATEWAIT(JA)=HATE(JA-1)
      PIGSCPHS=PHS(JA-1)
      INIZ=((W16/D11)*WAT)
      W=RATE(JA-1)+D1W
      10 JF (WP-CHG) 11,A0,0H0
      A0 JN01=U
      60 IN 12
    11 INITZEM=H0*HAE
      HP=HP+(INUDT*.000025)
  )2 VEL1=VFL2
      WTM=(VFL2*VEL2)/(GAMA*32.17*FIMP*PIT)
      MONT=1.0/11.0*((GAMA-1.0)/2.0)*W(MV)
      TUT=H00T*TAI
      PHFX=CPHS*TUT
      AC=)
      50 IF(VFL(K0)-VEL2)51,52,53
      51 K0=K0+1
      60 TO 50
  52 FACEPSY(K0)
      60 TO 59
  53 HAG=(VFL2-VEF(K0-1))/(VEE(K0)-VEE(K0-1))
      PFAC=((PSY(K0)-PSY(K0-1))*HAG)*PSY(K0-1)
  54 FM=(SHOT*(CHG/PFAC))/32.17
      ACFL=PMEX*AHEA*32.17*SHOT
      VEL2=VFL1*(ACEL*.000025)
      ACOL=(ACEL*.000025)/2.
      HINC=(VEL1*.000025)*(ACUL*.000025)
      MDT$MINIS*(HINC*12.)
  55 AVNL=CVOL*(H11S*AREA)
      DLT=VFL2
      UHW=(CHG-HP)/WH1
      COVL=CVL*HP
      INPT=((UNIDT*FIMP*12.0)-(GAMH*EFH*ACEL*VEL2*12.0)+(AREAPREX*VEL1*12
      1.0))/((AVOL-(UHW*CIVL))*
      INPT=J
      TIME=DOME*.000025
      FP1=HP/CHG
      IF(CPMS.GT.P10P) PTUP=CPHS
      WHT=(A,17)*IMP*CPHS*B015*FPU*0H1*UDOT*PREX
      15
      45

```

```

90      15 WRITE(6,17)LMF,CPHS,BDIS,FPU,OPUI,OLDT,PRES
91      17 FORMAT(F15.4,F15.1,F15.3,F15.4,F15.1,F15.2,F10.1)
92      NPTS=NPTS+1
93      PCPHS(NPTS)=CPHS
94      PHNTS(NPTS)=HNTS
95      CPRAZCPHS((INPUT*.00025)
96      IF (IND).GE.,HUN) GO TO 79
97      CONTINUE
98      79 DFLY=VEL2-VEL1
99      OWNEMENTS-HUN
100     ADV=(1.-10UN/(HINC*12.0))*DELV
101     AN=(VME*VM/HUN)*SMOT*(AREA*64.0)
102     WRITE(6,40)AN
103     FORMAT(//,25H PIEZOMETRIC PRESSURE IS ,F9.2,/)
104     WRITE(6,41)VM
105     FORMAT(//14H M/S//16H FEET PER SECOND//)
106     AHEAN/P1UP
107     AHEAM*100.
108     WRITE(6,42)AF
109     FORMAT(//26H PIEZOMETRIC EFFICIENCY IS,F7.1,0H PERCENT)
110     AH=(AF*EFM*32.17)/SHOT
111     FKFS=(VM*VM*SMOT)/(2.*32.*17)
112     TEZCHG*FIMP/(GAMA-1.)
113     HESTKT/TE*100.
114     WRITE(6,43)AH
115     FORMAT(//36H CROWNED PIEZOMETRIC EFFICIENCY IS,F7.1,0H PERCENT)
116     WRITE(6,44)HE
117     FORMAT(//24H BALLISTIC EFFICIENCY IS,F8.1,0H PERCENT)
118     CALL,MPLOT
119     GO TO 4
120     END
121     *14FTC HPI,OI
122     SUBROUTINE MPLOT
123     COMMON/ /PCPHS(1000),PHUIS(1000),HUN,P1TOP,NPTS
124     I=0
125     XL=PHUIS(I)
126     XH=PHUIS(NPTS)
127     YH=PCPHS(I)
128     P0958 00126
129     P0958 00127
130     P0958 00128
131     P0958 00129
132     P0958 00130
133     P0958 00131
134     P0958 00132
135     P0958 00133
136     P0958 00134
137     P0958 00135
138     P0958 00136
139     P0958 00137
140     P0958 00138
141     P0958 00139
142     P0958 00140
143     P0958 00141
144     P0958 00142
145     P0958 00143
146     P0958 00144
147     P0958 00145
148     P0958 00146
149     P0958 00147
150     P0958 00148
151     P0958 00149
152     P0958 00150
153
154     CALL GRIDLV(L,XL,YB,YT,DX,UY,N,M,I,J,NX,NY)
155     CALL PRINTV(-4,4MDIS,500,10)
156     CALL APINTV(0,-140,-444,CPHS,10,500)
157     CALL APLTV(NPTS,PT(1),PH1(1),I1*1*1*55,IERR)
158     CALL APLTV(NPTS,PT(1),PH2(1),I1*1*1*38,IERR)
159     I1=X1*X1*MDIS(1)
160     IY1=Y1*Y1*(PCPHS(1))
161     DO 300 IKK=2,NPTS
162     IX2=NAV(IPDIS(IKK))
163     IY2=NAV(IPDIS(IKK))
164     CALL LINEV(IX1,IY1,IX2,IY2)
165     IX1=IX1+2
166     IY1=IY2
167     CONTINUE
168     RETURN
169     END

```

(The reverse of this page is blank.)

SECTION IV

EXPERIMENTAL RESULTS

NORMAL DEFLAGRATION

The validity of the preceding analysis is easily assessed by measuring the pressure-time history and muzzle velocity of a given device and correlating the results with those predicted by the theory. This experimental effort was conducted at the Jet Propulsion Laboratory of the California Institute of Technology under NASA sponsorship. The device which was used for this purpose is shown in Figure 7.

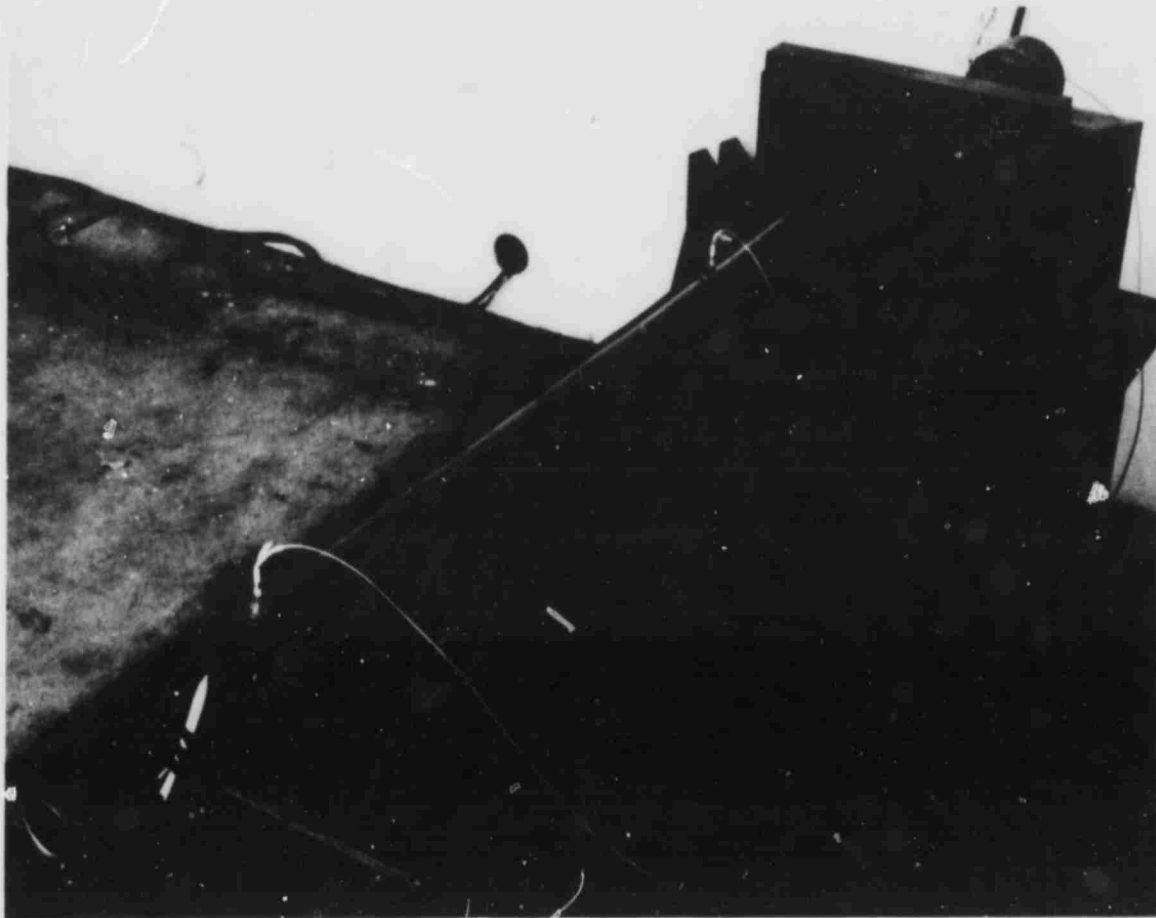


Figure 7. Device to Measure Pressure-Time History and Muzzle Velocity.

Pressures were measured in the chamber and at two additional points down the barrel by means of high-pressure Kistler piezometric pressure transducers feeding Kistler charge amplifiers and recorded on persistent phosphor Techtronix oscilloscopes. Muzzle velocities were measured by means of break screens connected to Hewlett-Packard digital clocks.

The launch tube was of smooth bore configuration and for maximum flexibility was constructed with a uniform bore diameter rather than with an expanded chamber; this design allows an infinitely variable chamber volume. Ignition and propellant loading techniques are shown in Figure 8.

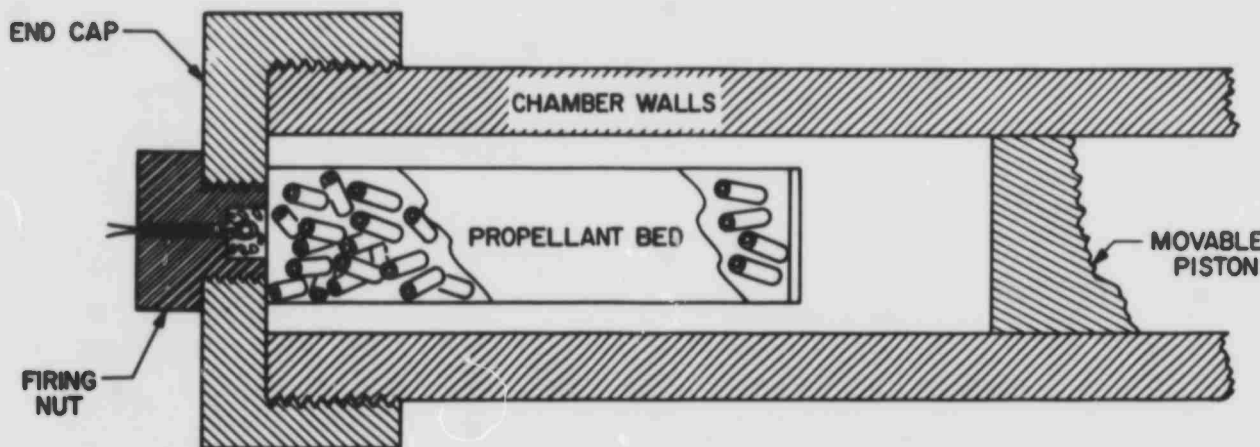


Figure 8. Ignition and Propellant Loading Techniques.

The initial chamber volume is determined by the location of the piston base while the loading volume is a function of the diameter and length of the phenolic sleeve into which the propellant is initially packed. The ignitor used consists of a firing nut containing an Atlas electric match surrounded by 300 mg of black powder. This type igniter gives a short-duration flame of high intensity with little brisance. When the tubular propellant grains are not too tightly packed, the effect of the phenolic loading sleeve may be neglected except insofar as the volume it displaces is concerned.

Firings demonstrating proper deflagration and typical correlation with the above referenced theory are illustrated in Figures 9, 10, and

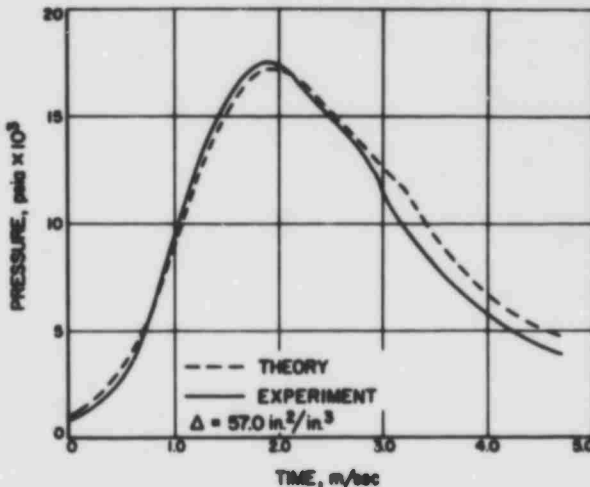


Figure 9. Pressure Time Plot With $\Delta = 57.0 \text{ in.}^3/\text{in.}^3$.

11. A qualitative delineation of the phenomena occurring in Figure 9, for example, would be as follows:

1. $t = 0$ to $t = 1.0 \text{ m/sec}$: Very slow increase in chamber volume as the result of an almost negligible projectile velocity, hence very rapid pressure increase due to energy release by propellant in almost constant chamber volume.

2. $t = 1.0 \text{ m/sec}$ to $t = 1.9 \text{ m/sec}$: Projectile velocity increasing and, thus, exposed chamber volume increasing more rapidly. Excess energy input decreasing as function of incremental volume to be pressurized.

3. Peak pressure ($t = 1.9$) to propellant burnout ($t = 2.9$ experimentally, 3.2 analytically): Plenum volume increasing more rapidly than energy input. Sharp break in curve slope due to propellant burnout.

4. Subsequent to burnout, a very rapid pressure decrease occurs as a result of the expansion of the gases, heat loss to tube, and further energy imparted to projectile.

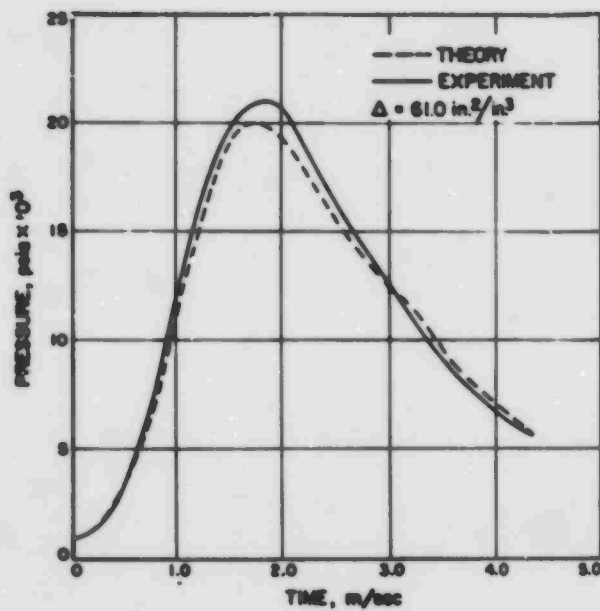


Figure 10. Pressure Time Plot With $\Delta = 61.0 \text{ in.}^2/\text{in.}^3$.

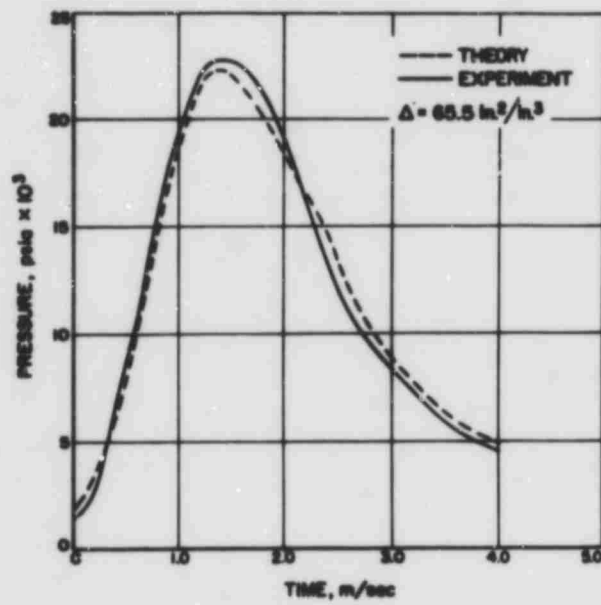


Figure 11. Pressure Time Plot With $\Delta = 65.5 \text{ in.}^2/\text{in.}^3$.

In these three firings, the primary difference exhibited between the experimental data and the analysis is a result of the following factor: the single-perforate propellant is assumed to burn externally and internally in a radial manner until the total charge is consumed.

In reality, this does not occur. A certain fraction of the grains fragment during combustion, and this increases the exposed burning surface and, in general, leads to slightly higher peak pressures and somewhat earlier web burnout than is analytically predicted. The difference, typically, is of only a few percent in peak pressure and is of such a nature that there is no way to express it analytically.

Figures 9, 10, and 11 show the quite good correlation between theory and experiment which is attainable when the density of loading Δ is kept at less than $75 \text{ in.}^2/\text{in.}^3$. At loadings above this level, a different mechanism of combustion becomes manifest and could probably be best described as a transition through shock-driven deflagration to virtual charge detonation. The charge characteristics are presented in Table V.

TABLE V. CHARGE CHARACTERISTICS.

Plot References	Charge Weight (gm)	Propellant Web (in.)	Slug Weight (gm)	Δ (in. ² /in. ³)	Muzzle Velocity (fps)	
					Predicted	Actual
Figure 9	86.2	0.0164	560	57.0	2,080	2,040
Figure 10	90.0	0.0164	560	61.0	2,220	2,210
Figure 11	110.0	0.0190	508	65.5	2,360	2,300
Figure 12	97.5	0.0164	560	76.7	2,250	2,150
Figure 13	93.0	0.0164	550	80.0	2,190	2,220
Figure 14	105.0	0.0164	560	82.0	2,350	2,700

SHOCK-DRIVEN DEFLAGRATION

It was mentioned previously that the phenolic tube had no effect on the interior ballistic solution. This is not true, however, if the propellant is packed too tightly into the tube. The propellant used was M-10, which is virtually 100 percent nitrocellulose with no nitroglycerine

loading and, hence, would be expected to be relatively insensitive to detonation characteristics.

Figures 12, 13, and 14 show this phenomenon of transition from weak shock-driven deflagration to strongly shock-driven deflagration. Figure 15 shows the remains of an end cap when loading was increased to the point where a response similar to complete detonation occurred. No pressure record is available for this firing because the breech pressure transducer was also destroyed. An indirect method of pressure determination may be made by the calculation of the force necessary to shear the normalized 4130 end cap and indicates a peak pressure of at least 450,000 psig.

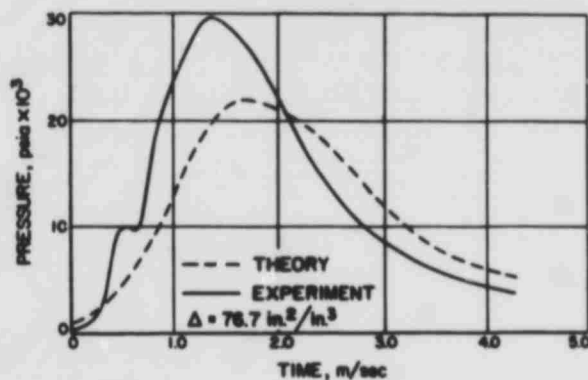


Figure 12. Pressure Time Plot With $\Delta = 76.7 \text{ in.}^2/\text{in.}^3$.

From the illustrated firings, it is possible to characterize the combustion of the propellant into various regimes as a function of the burning surface per unit of free initial volume. Symbolically, this would be

$$\Delta = S_B/V_{IF}$$

as

$$S_B = 2 C_w / \rho_p w_0$$

then

$$V_{IF} = L A_p - C_w / \rho_p$$

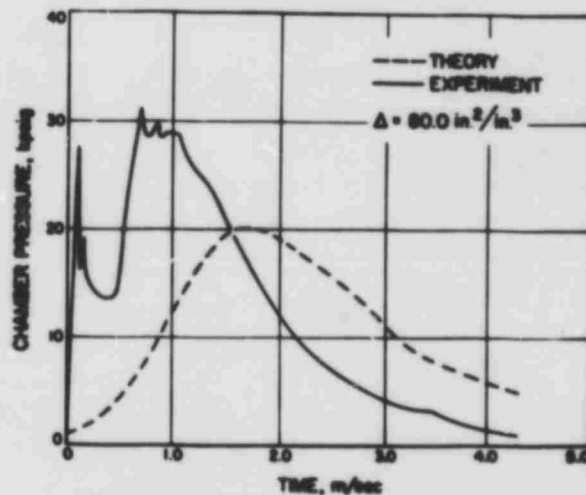


Figure 13. Pressure Time Plot With $\Delta = 80.0 \text{ in.}^2/\text{in.}^3$.

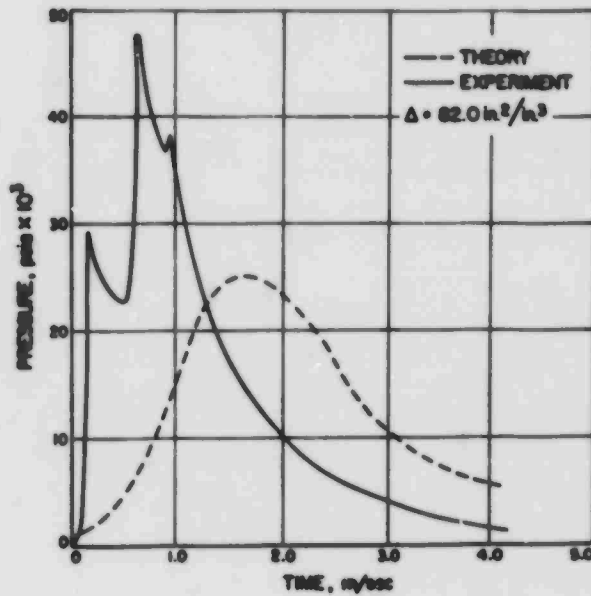


Figure 14. Pressure Time Plot With $\Delta = 82.0 \text{ in.}^2/\text{in.}^3$.

It was mentioned earlier that, for proper deflagration in this system, Δ must be less than $75 \text{ in.}^2/\text{in.}^3$. In Figure 12, $\Delta = 76.7 \text{ in.}^2/\text{in.}^3$ and it was seen that a slight pressure pulse occurs, then damps out, but drives the peak pressure to a value approximately 30 percent higher than what would have been encountered during proper deflagration.

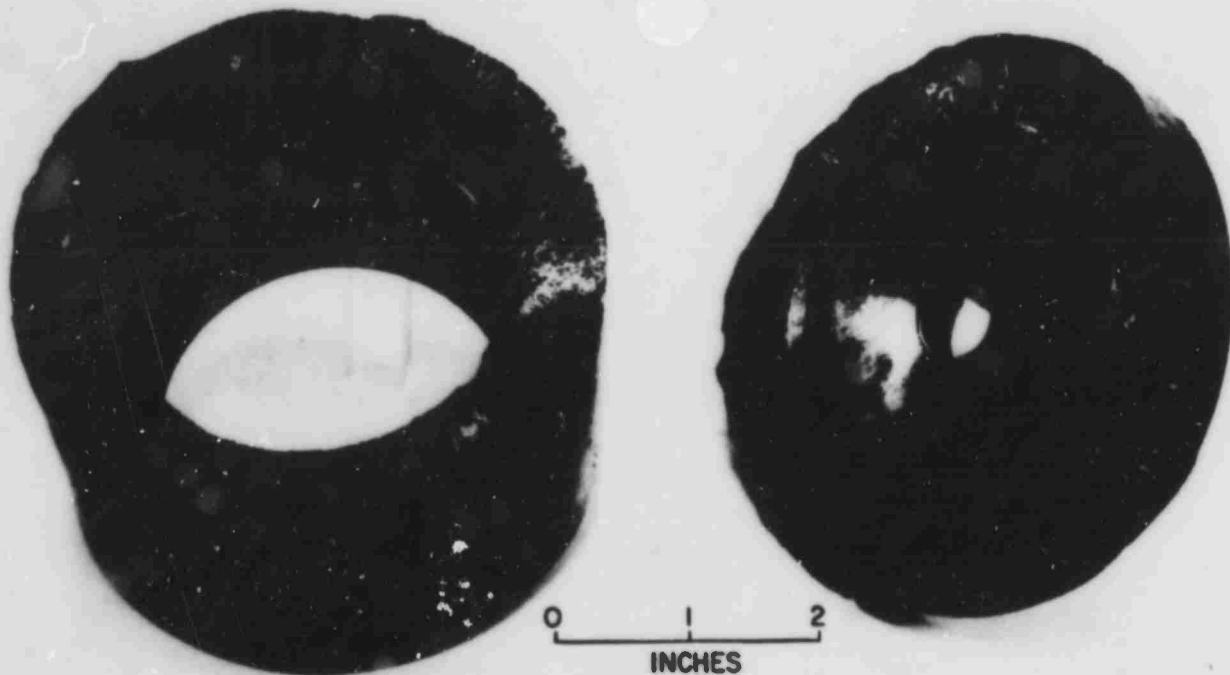


Figure 15. End Cap After Detonative Reaction.

In Figure 13, for which $\Delta = 80 \text{ in.}^2/\text{in.}^3$, the initial pressure spike is rapid and narrow and quickly decays to be followed by another broader pressure pulse to approximately the same value. Figure 14 shows the pressure-time profile of a loading with a $\Delta = 82 \text{ in.}^2/\text{in.}^3$.

The initial pressure wave is virtually identical to that exhibited by the previous loading. The second spike, however, is much higher and gives a peak pressure almost 100 percent higher than would be expected if linear regression were the only mechanism at work.

The loading represented by the wreckage shown in Figure 15 was $\Delta = 86.5 \text{ in.}^2/\text{in.}^3$. A detonation-like reaction phenomenon had occurred, resulting in a pressure probably well above the 450,000 psig mentioned previously. The response could have been a true detonation of the individual propellant grains, which then formed a gaseous blast over-pressure wave to act on the restraining steel. The energy release rate was such that this is the most likely mode of reaction.

The Δ values given for the onset of this highly undesirable mode of reaction would include most fully loaded cartridge cases with thin web propellant. This demonstrates the requirements for either deterring or inhibiting a large fraction of the initial surface area. Good ballistic design, however, requires a tradeoff between reproducible ignition and the formation of these dangerous shock waves in the deflagrating propellant bed.

From the previous results for the system under consideration, the following regimes can be defined:

$\Delta < 75$	Proper deflagration
$75 < \Delta < 86$	Shock-driven deflagration
$\Delta > 86$	Detonation like response

These particular Δ values are doubtless a function of propellant composition and ignition technique. They do graphically demonstrate, however, that the ballistic designer must be cautious when approaching very high loading densities to be certain that the regimes, other than normal propellant regression, are avoided.

REFERENCES

1. Heiney, O.K., "Simplified Interior Ballistics of Propellant Actuated Devices," JPL SPS 47-43.
2. Corner, J., "Theory of the Interior Ballistics of Guns," John Wiley, New York, 1950.
3. Hirschfelder, Kershner, and Curtiss, "Interior Ballistics," Volumes I and II, February and April 1943, NDRC Reports A-142 and A-180 (declassified).
4. Kent, R. H., "Some Special Solutions for the Motion of the Powder Gas," Physics 7, 1936.
5. NACA Report 1135, "Equations, Tables and Charts for Compressible Flow," 1953.
6. Serebryakov, M.E., "Interior Ballistics," Moscow 1949, translated at Catholic University of America under Contract NORD 10, 260
7. CPIA, "Solid Propellant Manual," Chemical Propulsion Information Agency, Johns Hopkins University, Silver Spring, Md, 1965 (Confidential).
8. "Internal Ballistics," Philosophical Library, New York, 1951.
9. "Interior Ballistics of Guns," U. S. Army Materiel Command Pamphlet 706-150, February 1965.
10. Heiney, O.K., "A New Computer-Oriented Formulism for Gun Ballistics," Volume II, 3rd ICRPG/AIAA Solid Propulsion Conference Proceedings, CPIA Publication, April 1968.

UNCLASSIFIED

Security Classification

DOCUMENT CONTROL DATA - R & D

(Security classification of title, body of abstract and indexing annotation must be entered when the overall report is classified)

1. ORIGINATING ACTIVITY (Corporate author) Air Force Armament Laboratory Air Force Systems Command Eglin Air Force Base, Florida	2a. REPORT SECURITY CLASSIFICATION UNCLASSIFIED
3. REPORT TITLE ANALYTIC AND EXPERIMENTAL INTERIOR BALLISTICS OF CLOSED BREECH GUNS	2b. GROUP

4. DESCRIPTIVE NOTES (Type of report and inclusive dates) Final Report
--

5. AUTHOR(S) (First name, middle initial, last name) Heiney, Otto K., 1st Lt, USAFR

6. REPORT DATE May 1969	7a. TOTAL NO. OF PAGES 46	7b. NO. OF REFS 10
8a. CONTRACT OR GRANT NO. <i>H/K</i> 62405094-2560	8b. ORIGINATOR'S REPORT NUMBER(S) AFATL-TR-69-42	
c.	8c. OTHER REPORT NO(S) (Any other numbers that may be assigned this report)	
d.		

10. DISTRIBUTION STATEMENT This document is subject to special export controls, and each transmittal to foreign nationals or foreign governments may be made only with prior approval of the Air Force Armament Laboratory (ATWG), Eglin Air Force Base, Florida 32542.		
---	--	--

11. SUPPLEMENTARY NOTES Available in DDC	12. SPONSORING MILITARY ACTIVITY Air Force Systems Command Andrews AFB, Wash, DC 20331
--	--

13. ABSTRACT A closed breech incremental interior ballistic formulism is presented along with a Fortran 4 computer program which utilizes the system. Typical input and output data, both plotted and tabular, are included. A unique characteristic of the system is that it avoids the inaccuracies associated with approximate analytic propellant regression expressions in that regression rates are determined by a tabular routine. Various pressure gradient expressions are investigated. Correlation of the mathematical model and computer predictions to experimental device firings are presented. A shock-driven deflagration effect which may be initiated during the ignition transient is described and a postulated correlation parameter defined.		
---	--	--

Interior ballistics
Ammunition propellants
Guns

UNCLASSIFIED
Security Classification